PAPER

Check for updates

New Ag$_8$PtO$_6$: synthesis, crystal structure, physical properties and theoretical analyses†

Gohil Singh Thakur, [ID] [a] Hans Reuter, [ID] [b] Helge Rosner,[a] Gerhard H. Fecher, [ID] [a] Claudia Felser[a] and Martin Jansen [ID] *[a,c]

We report the synthesis, crystal structure, and basic physical properties of Ag$_8$PtO$_6$, which represents the first silver platinum ternary oxide. The crystalline compound was obtained from appropriate mixtures of the binary constituents under alkaline conditions at high oxygen pressure, while applying relatively mild thermal conditions (573 K). Ag$_8$PtO$_6$ crystallizes in a new crystal structure in the triclinic system ($P\bar{1}$). The structure consists of slightly distorted, discrete PtO$_6$ octahedra, which are linked *via* O−Ag−O dumbbells to form a three dimensional framework. It is a diamagnetic semiconductor with a band gap of 0.9 eV. DFT based calculations confirm an electronic ground state that corresponds to a 5d^6 6s^0 configuration of the Pt atoms, in accordance with the observed diamagnetism.

Introduction

The terrestrial abundance of the platinum group elements (PGEs) is quite low. However, this class of transition metals continues to play a prominent role in science and technology.[1] Alloys based on such constituents are among the thermally and chemically most durable metallic structural materials.[2] Catalysts, with PGEs as constituents, employed in large scale chemical production,[3] for exhaust gas purification[4] or in fuel cells[5] are legendary, not to mention *cis*-platinum complexes in use as cancer drugs.[6,7] In science, *e.g.*, complexes of PGE helped to bring coordination chemistry as a new sub-discipline of inorganic chemistry to birth,[8] or the so-called Krogmann's salts[9] attracted considerable attention during at least two decades in the second half of the last century. In current condensed matter research, discovery of exotic electronic phases prevailing in certain PGE oxides has stimulated vibrant activity. Here, as a common thread, Hund's coupling, spin orbit coupling (SOC), crystal field (CF) splitting, hopping integrals, and electron correlations (U_H) are energetically on a comparable scale, thus giving rise to diverse uncommon electronic and/or magnetic ground states.[10,11]

Most of the phases so far studied represent ternary oxides of PGEs and group I and II elements. Monovalent cations of group XI, Cu^{1+} and Ag^{1+}, which are known to interrupt or at least to weaken magnetic exchange paths, have attracted much less interest, yet. Aiming at keeping the electronic effects mentioned above as localized as possible by suppressing long range hopping, we started to explore the ternary systems spanned by silver(I) oxides and PGEs.

Here we report on Ag$_8$PtO$_6$, the first silver oxo-platinate, its crystal structure and basic physical properties. In our computational analyses, we place particular emphasis on the nature of the electronic ground state, which one would conventionally associate with a low spin 5d^6, t$_{2g}$^{6} configuration. However, due to relativistic contraction of the 6s orbitals, states derived from the 6s^2, 5d^4 (t$_{2g}$^{4}) configuration might be lower in energy and give rise to a J_{eff} = 0 scenario, as encountered *e.g.* with Ir^{5+} oxides.[12] Applying density functional band structure calculations, we can clearly assign a 5d^6 6s^0 configuration to the Pt atoms, consistent with a non-magnetic state.

Experimental section

Single crystal synthesis

Single crystals of Ag$_8$PtO$_6$ were prepared by reacting Ag$_2$O and PtO$_2$, 0.257 g and 0.0631 g, respectively, as a typical batch composition, in an alkaline medium at 573 K and under high oxygen pressure in a steel autoclave. Ag$_2$O was pre-synthesized by precipitating from an aqueous solution of AgNO$_3$ with an excess of NaOH. PtO$_2$ was used as purchased (Sigma Aldrich, 99.9%) without any further purification. Well ground mixtures of the oxides were placed in a gold crucible of ~4 cm height, welded from one end and mechanically crimped from the other. About 1.5 ml of 3 M KOH was used as a mineralizer to

[a]Max-Planck-Institut für Chemische Physik fester Stoffe, Nöthnitzer Straße 40, 01187 Dresden, Germany
[b]Institut für Chemie neuer Materialien, Universität Osnabrück, Barbarastraße 7, 49069 Osnabrück, Germany
[c]Max-Planck-Institut für Festkörperforschung, Heisenbergstr. 1, 70569 Stuttgart, Germany. E-mail: M.Jansen@fkf.mpg.de
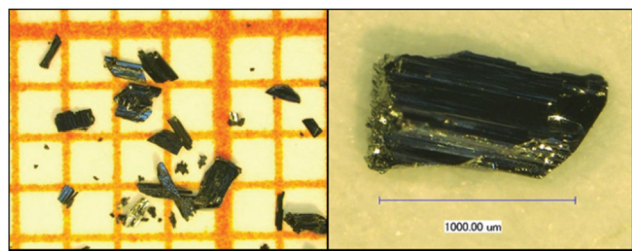†Electronic supplementary information (ESI) available. See DOI: 10.1039/c8dt05081c

Fig. 1 Photographs of few single crystals of Ag_8PtO_6, left: on a millimeter grid.

promote crystal growth. The crucible was placed in a 20 ml stainless steel autoclave[13] and about 11.2 ml of liquid oxygen was condensed in it. The gas-tight sealed autoclave was heated at 573 K in a vertical furnace for 96 hours and cooled slowly to room temperature in about 24 hours. The O_2 pressure generated in the autoclave at this temperature is estimated to be around 250 MPa. Large corrugated plate-like shiny black single crystals of maximum length ~1.2 mm (see Fig. 1) were obtained along with small amounts of tiny polygonal crystals of Ag_2O. The crystals were easily handpicked and sonicated in ethanol to remove any surface impurities. The crystalline product is insensitive to air and moisture.

Instruments for physical property measurements

Thermogravimetric (TGA) analysis of Ag_8PtO_6 was carried out on a Netzsch STA 449 C analyzer. About 30 mg of the sample was placed in a corundum crucible, which was heated and subsequently cooled at a rate of 5 K min^{-1} in the range of 300–1273 K under dynamic argon flow.

Susceptibility of crushed single crystals was measured in applied magnetic fields up to $\mu_0H = 7$ T and in the temperature range between 2 and 400 K in a MPMS-XL7 magnetometer (Quantum Design).

Temperature dependent resistivity was measured on a plate-like single crystal of dimension $0.6 \times 0.15 \times 0.025$ mm^3 by a two-probe method in a PPMS instrument (Quantum Design).

Structure determination and refinement

A black plate-like crystal fragment of appropriate size was obtained by cutting a larger crystal under a microscope. It was fixed on a 50 micron Micromesh MiTeGen Micromount using FROMBLIN Y perflouropolyether (LVAC 16/6, Sigma-Aldrich). Diffraction data were collected at ambient temperature on a Bruker Kappa APEX II CCD-based 4-circle X-ray diffractometer using graphite monochromated MoKα radiation (λ = 0.71073 Å) of a fine focus molybdenum target X-ray tube operating at 50 kV and 30 mA. Collection and reduction of data were carried out with the Bruker Suite software package.[14] Intensities were corrected for absorption effects semi-empirically from equivalents via SADABS.[15] The structure was solved by direct methods and refined by full-matrix least-squares fitting on F^2 with the SHELXL software package.[16,17] Figures were drawn using DIAMOND.[18]

Table 1 Crystal and structure refinement data for Ag_8PtO_6

Formula	Ag_8O_6Pt
Fw	1154.05 (g mol^{-1})
T/K	296(2)
λ/Å	0.71073
Space group	$P\bar{1}$
a/Å	6.1911(2)
b/Å	6.9665(2)
c/Å	10.3901(3)
α/°	87.396(1)
β/°	85.152(1)
γ/°	71.751(1)
V/Å^3	423.98(2) Å^3
Z	2
Calc. d/g cm^{-3}	9.04
μ(Mo-Kα)/mm^{-1}	34.471
$F(000)$	1004
Crystal size	$0.167 \times 0.067 \times 0.035$ mm
Theta range for data collection	3.079° to 29.991°.
Reflections collected/unique	75 196/2467 [R(int) = 0.0495]
Completeness to theta = 25.242	99.9%
Absorption correction	Semi-empirical from equivalents
Refinement method	Full-matrix least squares on F^2
Data/restraints/parameters	2467/0/140
R_1/wR_2 [all data]	0.0135/0.0282
R_1/wR_2 [$I > 2\sigma(I)$]	0.0137/0.0283
Extinction coefficient	0.00371(6)
Largest diff. peak/hole	1.096/−1.067 e/Å^3

Table 2 Atomic coordinates ($\times 10^{-4}$) and equivalent isotropic displacement parameters (Å$^2 \times 10^{-3}$) for Ag_8PtO_6. U(eq) is defined as one third of the trace of the orthogonalized U_{ij} tensor

Atom	x	y	z	U(eq)
Ag(1)	5000	0	5000	4(1)
Ag(2)	1528(1)	3618(1)	4037(1)	5(1)
Ag(3)	4589(1)	7214(1)	388(1)	6(1)
Ag(4)	3812(1)	6666(1)	4016(1)	6(1)
Ag(5)	1585(1)	4657(1)	1343(1)	5(1)
Ag(6)	−1482(1)	7639(1)	3046(1)	6(1)
Ag(7)	−1378(1)	8746(1)	311(1)	5(1)
Ag(8)	0	0	5000	5(1)
Ag(9)	3052(1)	10 319(1)	2278(1)	5(1)
Pt(1)	7132(1)	2898(1)	2458(1)	3(1)
O(1)	5185(5)	2617(4)	4074(3)	5(1)
O(2)	8931(5)	3463(4)	870(3)	6(1)
O(3)	4480(5)	5361(4)	2052(3)	6(1)
O(4)	8087(5)	4724(4)	3578(3)	5(1)
O(5)	6038(5)	1025(4)	1418(3)	6(1)
O(6)	9615(5)	356(4)	2952(3)	6(1)

Crystallographic data, details of data collection and structure refinement are given in Table 1, atomic coordinates, and equivalent isotropic displacement parameters in Table 2, bond lengths in Table S1† and anisotropic displacement parameters Table S2 in the ESI.†

Further details of the crystal structure investigation may be obtained from FIZ Karlsruhe, 76344 Eggenstein-Leopoldshafen, Germany (fax: (+49)7247-808-666; email: crysdata(at)fiz-karlsruhe(dot)de, on quoting the deposition number CSD 434624. During all final calculations, the lattice parameters as obtained from X-ray powder pattern refinement were used.

Laboratory powder X-ray diffraction (PXRD) data (Fig. 2) were collected at room temperature on a HUBER G670 imaging
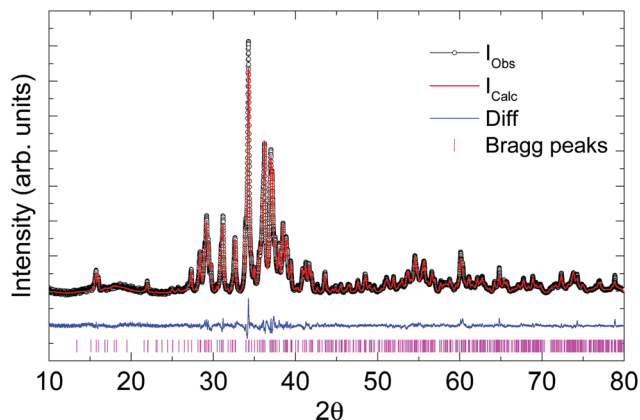
Fig. 2 Le Bail fit of the powder X-ray diffraction data of Ag_8PtO_6 collected at 300 K.

plate Guinier camera with Cu-Kα_1 radiation (λ = 1.5406 Å), in a 2θ range of 10–80 degrees. Rietveld refinement and Le Bail fitting were carried out with the TOPAS-4.2.0.2 (AXS) program.[19] The refined parameters were the scale factor, zero point of θ, sample displacement (mm), background as a Chebyshev polynomial of 20th degree, $1/x$ function, crystallite size, micro-strain and cell constants.

Theoretical calculations

Relativistic density functional (DFT) electronic structure calculations were performed using the full-potential FPLO code, version fplo18.00-52.[20] For the exchange–correlation potential, within the general gradient approximation (GGA), the parametrization of Perdew–Burke–Ernzerhof was chosen.[21]

The spin–orbit (SO) coupling was treated non-perturbatively solving the four component Kohn–Sham–Dirac equation.[22] To obtain precise band structure information, the calculations were carried out on a well converged mesh of 600 k-points ($10 \times 10 \times 6$).

To test the reliability of the calculations, the internal positions of the atoms were optimized by minimizing forces with remaining forces smaller than 0.05 eV Å^{-1}. For the shown electronic density of states, (DOS) the experimental crystal structure has been used.

Results and discussion

New Ag_8PtO_6 has been obtained from the binary constituent oxides under hydrothermal conditions, applying an elevated oxygen pressure of 250 MPa, however, rather mild thermal conditions of 573 K. It starts decomposing at about 673 K, loosing oxygen in a few steps and being completely reduced upon heating to 873 K, see Fig. S1 in the ESI.† The total weight loss is about 8.5% corresponding to complete loss of oxygen. The remaining product is a mixture of the constituent metals Ag and Pt.

The title compound crystallizes in a triclinic system with space group $P\bar{1}$, cf. Tables 1 and 2. The unique crystal structure
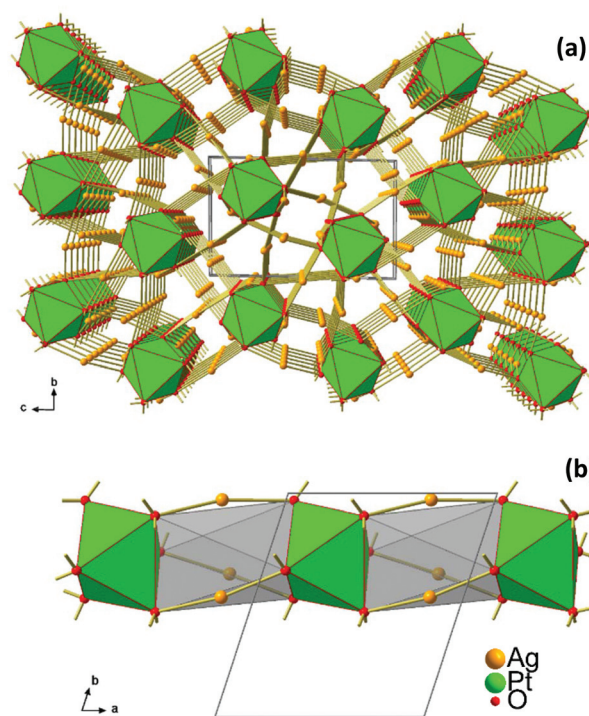

Fig. 3 (a) Crystal structure of Ag_8PtO_6 viewed along the a-axis, (b) 1D stack of PtO_6 octahedra extending along [100].

consists of discrete, virtually ideal PtO_6 octahedra and linear, or slightly bent, respectively, AgO_2 dumbbells (Fig. 3). The primary PtO_6 structural units are linked by silver atoms in twofold coordination to form a three-dimensional framework structure. Oxygen is found in two different structural functions, μ_3 and μ_4, connecting either one platinum atom with two (O2 and O4) or three (O1, O3, O5, and O6) silver atoms, respectively. As a result, each PtO_6 octahedron is connected to nine other surrounding octahedra through sixteen O–Ag–O linkages (Fig. 4).

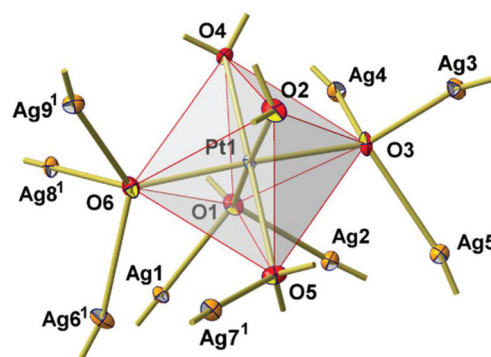The Ag–O bond lengths range from 2.04 to 2.26 Å (Table S1†) and agree well with the values reported in the

Fig. 4 Primary PtO_6 structural unit with connected AgO_2 dumbbells. All atoms are drawn as thermal displacement ellipsoid at the 40% probability level. Symmetry code to generate equivalent atoms: (1) $1 + x$, $-1 + y$, z.

literature for Ag–O bonds.[23–25] The Pt–O bond lengths vary in the narrow range of 1.99 to 2.03 Å (Table S1†) which are also in excellent agreement with other reported oxides with Pt in +4 oxidation.[26–28] The shortest Ag–Ag distance is 2.85 Å (Ag3–Ag5) which is slightly shorter than that of the nearest neighbour distances in Ag metal (2.89 Å); this separation, and in addition those extending up to 2.95 Å, are indicative of the presence of weakly bonding d^{10}–d^{10} interactions.[29] At a first glance, the structure appears to be rather open; however, the calculated free volume amounts to only 11.8 Å^3 or 8%.[30]

Interestingly, in spite of the underlying overall three dimensional connectivity pattern some eye catching one dimensional structural anisotropy is becoming apparent when viewing the crystal structure in the [100] direction, see Fig. 3a. In this perspective the octahedra appear to be stacked in a staggered fashion, like a column excised from a hcp packing of oxygen atoms where every second octahedral void is centred by platinum, while the empty ones are bridged by silver atoms, see Fig. 3b. This particular microscopic feature seems to reflect the fibrous appearance of the crystals' surface.

Ag_8PtO_6 is semiconducting with an activated type behavior in the temperature range 400 K to 280 K with room temperature resistivity of the order of 50 kΩ cm (Fig. 5a). The

Arrhenius fit in the high temperature region yields a band gap of 0.89 eV, which falls in line with the observed semiconducting nature of the sample.

The compound is found to be diamagnetic in the entire temperature region studied from 360 K to 2 K, (Fig. 5b). The susceptibility is negative and temperature independent in the high temperature region from 360 to 50 K, below which a weak field dependent Curie–Weiss like behavior is observed, which is due to the paramagnetic contribution of trace molecular oxygen impurity, which corresponds to a total of 0.7% of a spin $\frac{1}{2}$ species. The value of χ^∞ estimated from the extrapolation of Honda–Owen plots to infinite field comes out to be -224×10^{-6} emu mol^{-1}. The diamagnetic behavior is consistent with +4 oxidation state of Pt with all d-electrons paired as implied from the empirical formula.

In order to discriminate between the two possible diamagnetic ground states, as can be derived from the configurations $5d^6$ (t_{2g}^6), $S = 0$ and $6s^2$, $5d^4$ (t_{2g}^4), $J_{eff} = 0$, density functional band structure calculations have been performed. In a first step, we optimized the internal coordinates of the atomic positions with respect to the total energy, assuming the experimentally determined lattice parameters. As a result, we find a surprisingly good agreement of the experimentally refined and the calculated atomic positions, and changes of the Ag–O and Pt–O bond lengths are about 0.01 Å, only. The corresponding difference in total energy between both parameter sets yields 2.5 meV per atom, corresponding to a temperature of about 30 K. These findings provide independent strong support to the structural parameters from the XRD refinement.

Our calculations reveal that Ag_8PtO_6 is a narrow band gap semiconductor. The calculated band gap has a size of about 150 meV. No instability towards magnetism was found. These findings are consistent with the experimental observations. The experimentally observed gap of 0.9 eV is, however, significantly larger than the calculated one. This is in line with the usual underestimation of the electronic gap size applying standard DFT functionals.

The calculated electronic density of states is shown in Fig. 6 (upper panel). The valence band has a width of about 8 eV, typical of this type of oxide system. The density of states is dominated by the silver 4d bands that are concentrated in the energy range from −6 to −2 eV. The oxygen states are distributed rather uniformly across the complete valence bands. A more detailed analysis shows that these states are of rather different character. The states below −6 eV are bonding states derived from the Pt–O octahedra. Their counterpart is separated by a large covalency split of about 5 eV between −4 eV and the Fermi level at zero energy. The Pt states of the valence band are almost exclusively of 5d character (see Fig. 6, lower panel). They are found in three groups: at the bottom of the valence band below −6 eV, in the middle of the valence band, and close to the Fermi energy above −1.5 eV. The low and high lying states are hybridized with the oxygen states, originating from the covalent PtO_6 octahedra, whereas the states between −3.5 and −2 eV fall in the energy range where the majority of Ag 4d-states are located.
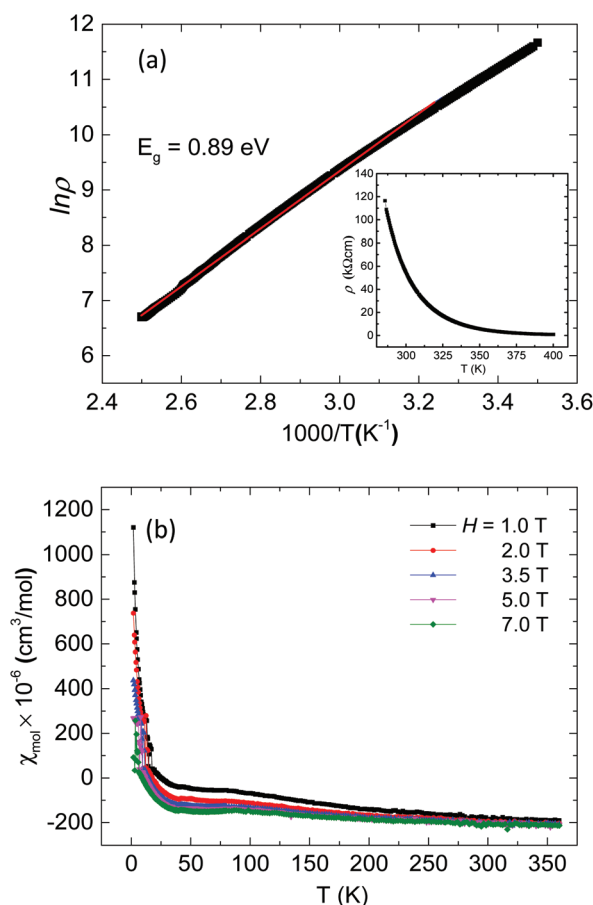

Fig. 5 (a) Arrhenius plot of resistivity of Ag_8PtO_6 with variable temperature resistivity in the inset (b) variable temperature susceptibility of Ag_8PtO_6 at various applied magnetic fields.
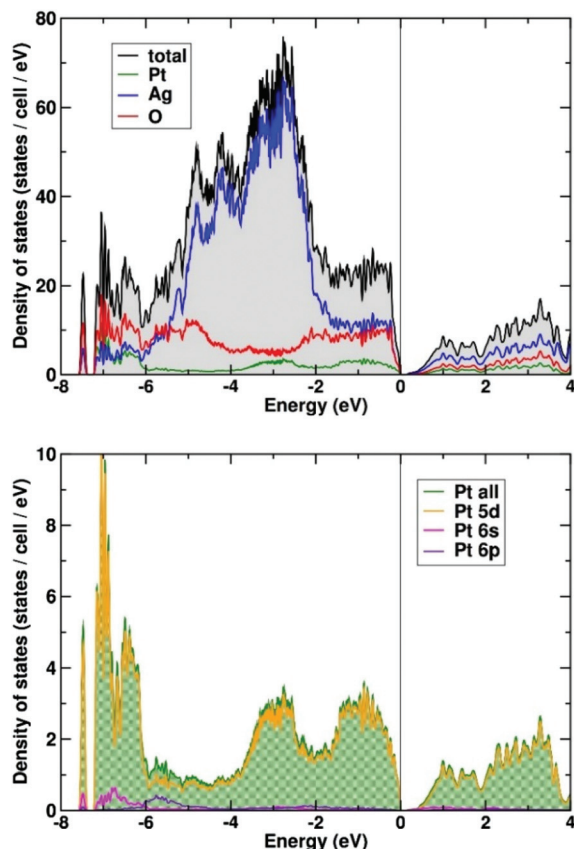
Fig. 6 Total and partial electronic density (DOS) of states of Ag_8PtO_6 (upper panel). The lower panel shows the orbital decomposed DOS of the Pt atom.

A small amount of Pt 6s (and 6p) states is found at the bottom of the valence band (see Fig. 6, lower panel). A population analysis shows that 6s states are occupied by about 0.15 electrons (on-site contribution). The majority of (unoccupied) Pt 6s states appear about 10 eV above the Fermi energy (not shown here).

The electronic ground state of Pt in Ag_8PtO_6 is $5d^6$, $6s^0$ in very good approximation. Thus, the findings are clearing the suspicion that the 6s might have submerged below the 5d states, as was found earlier for Cs_2Pt[31] and other platinides.[32]

Conclusions

A new silver-platinate, Ag_8PtO_6, has been synthesized as single crystals. This ternary oxide is inaccessible *via* solid state synthesis or solution chemistry, unless elevated oxygen pressure is applied, sufficiently high to suppress decomposition of the binary starting oxides. This finding is accentuating again the great potential of oxygen high pressure techniques for the synthesis of multinary oxide materials based on noble metals, be it in an explorative or purposeful approach. Such advanced preparation techniques have opened an entrance to a widely unexplored area of the energy landscape of chemical matter[33]

spanned *e.g.* by the oxides of PGEs and coinage metals. Compounds made of appropriate combinations of noble metals are offering interesting prospects for basic research as well as for applications. The title compound will for sure show activity as a heterogeneous catalyst, yet, its pertinent performance in comparison with catalysts actually in use needs to be checked.

The title compound crystalizes in a triclinic unit cell, and represents a new structure type. The structure consists of isolated PtO_6 octahedra connected by linear and/or slightly bent Ag–O linkages. It is found to be a diamagnetic semiconductor with an experimental band gap of ~0.9 eV. Band structure calculations clearly assign a $5d^6$ $6s^0$ state to the Pt atom, consistent with its non-magnetic state.

Conflicts of interest

There are no conflicts to declare.

Acknowledgements

References

1 *Gmelin Handbook of Inorganic and Organometallic Chemistry - 8th edition, Supplement Volume A 1 Technology of Platinum-Group Metals*, ed. G. J. K. Acres and K. Swars, Springer, Berlin Heidelberg, 1985.
2 A. S. Darling, *Platinum Metals Rev.*, 1960, **4**, 18–26.
3 J. E. Perea Buceta, I. Fernández, S. Heikkinen, K. Axenov, A. W. T. King, T. Niemi, M. Nieger, M. Leskelä and T. Repo, *Angew. Chem., Int. Ed.*, 2015, **54**, 14321–14325.
4 H. Hirata, *Catal. Surv. Asia*, 2014, **18**, 128–133.
5 Y. Bing, H. Liu, L. Zhang, D. Ghosh and J. Zhang, *Chem. Soc. Rev.*, 2010, **39**, 2184–2202.
6 B. Rosenberg, L. Van Camp, J. E. Trosko and V. H. Mansour, *Nature*, 1969, **222**, 385–386.
7 *CISPLATIN – Chemistry and Biochemistry of a Leading Anticancer Drug*, ed. B. Lippert, WILEY-VCH, Weinheim, 1999.
8 L. H. Gade, *Z. Anorg. Allg. Chem.*, 2012, **638**, 247–248.
9 H. Wagner, M. P. Geserich, R. V. Baltz and K. Krogmann, *Solid State Commun.*, 1973, **13**, 659–663.
10 Y. Tokura and N. Nagaosa, *Science*, 2000, **288**, 462–468.
11 S. V. Streltsov and D. I. Khomskii, *Phys.-Usp.*, 2017, **60**, 1121.
12 B. E. Prasad, Th. Doert, C. Felser and M. Jansen, *Chem. – Eur. J.*, 2018, **24**, 16762–16765.
13 C. Linke and M. Jansen, *Z. Anorg. Allg. Chem.*, 1997, **623**, 1441–1446.

14 *Bruker Suite, version 2013/1*, Bruker AXS Inc., Madison, WI, 2013.

15 G. M. Sheldrick, *SADABS —Bruker AXS area detector scaling and absorption, version 2012/1*, University of Göttingen, Germany, 2012.

16 G. M. Sheldrick, Short History of SHELX, *Acta Crystallogr., Sect. A: Found. Crystallogr.*, 2008, **64**, 112–122.

17 G. M. Sheldrick, Crystal Structure Refinement with SHELXL, *Acta Crystallogr., Sect. C: Struct. Chem.*, 2015, **71**, 3–8.

18 K. Brandenburg, *Diamond-Crystal and Molecular Visualization*, Crystal Impact, Bonn, Germany, 2006.

19 *TOPAS (version 4.2.0.2), General Profile and Structure Analysis Software for Powder Diffraction Data*, Bruker AXS GmbH, Karlsruhe (Germany), 2012.

20 K. Koepernik and H. Eschrig, *Phys. Rev. B: Condens. Matter Mater. Phys.*, 1999, **59**, 1743–1757; I. Opahle, K. Koepernik and H. Eschrig, *Phys. Rev. B: Condens. Matter Mater. Phys.*, 1999, **60**, 14035–14040 http://www.fplo.de.

21 J. P. Perdew, K. Burke and M. Ernzerhof, *Phys. Rev. Lett.*, 1996, **77**, 3865–3868.

22 H. Eschrig, M. Richter and I. Opahle, Relativistic Solid State Calculations, in *Relativistic Electronic Structure Theory, (Part II, Applications)*, ed. P. Schwerdtfeger, Theoretical and Computational Chemistry, Elsevier, 2004, vol. 13, p. 723.

23 S. Deibele, J. Curda, E.-M. Peters and M. Jansen, *Chem. Commun.*, 2000, 679–680.

24 J. Curda, W. Klein and M. Jansen, *J. Solid State Chem.*, 2001, **162**, 220–224.

25 S. Deibele and M. Jansen, *J. Solid State Chem.*, 1999, **147**, 117–121.

26 W. Urland and R. Hoppe, *Z. Anorg. Allg. Chem.*, 1972, **392**, 23–36.

27 J. J. Randall and L. Katz, *Acta Crystallogr.*, 1959, **12**, 519–521.

28 P. Kroeschell, R. Wolf and R. Hoppe, *Z. Anorg. Allg. Chem.*, 1986, **536**, 81–91.

29 M. Jansen, *Angew. Chem.*, 1987, **99**, 1136–1149, (*Angew. Chem., Int. Ed. Engl.*, 1987, **26**, 1098–1110).

30 Mercury CSD 2.0 - New Features for the Visualization and Investigation of Crystal Structures: C. F. Macrae, I. J. Bruno, J. A. Chisholm, P. R. Edgington, P. McCabe, E. Pidcock, L. Rodriguez-Monge, R. Taylor, J. van de Streek and P. A. Wood, *J. Appl. Crystallogr.*, 2008, **41**, 466–470.

31 A. S. Karpov, J. Nuss, U. Wedig and M. Jansen, *Angew. Chem.*, 2003, **115**, 4966–4969, (*Angew. Chem., Int. Ed. Engl.*, 2003, **42**, 4818–4821).

32 A. S. Karpov, J. Nuss, U. Wedig and M. Jansen, *J. Am. Chem. Soc.*, 2004, **126**, 14123–14128.

33 M. Jansen, *Angew. Chem.*, 2002, **114**, 3896–3917, (*Angew. Chem., Int. Ed. Engl.*, 2002, **41**, 3746–3766).